JOM Journal of Optical Microsystems

RESEARCH PAPER

Modeling holographic optical element performance with an extended source; experimental investigation using misaligned point sources

Jorge Lasarte,[a,b] Kevin Murphy,[a,b] Izabela Naydenova,[a,b] Jesús Atencia,[c] Maria Victoria Collados,[c] and Suzanne Martin*[,a,b]

[a]Technological University Dublin, School of Physics, Clinical and Optometric Sciences, Dublin, Ireland
[b]Technological University Dublin, Centre for Industrial and Engineering Optics, FOCAS Research Institute, Dublin, Ireland
[c]University of Zaragoza, Engineering Research Institute of Aragon (I3A), Zaragoza, Spain

ABSTRACT. Holographic optical elements (HOEs) have the potential to enable more compact, versatile, and lightweight optical designs, but many challenges remain. Volume HOEs have the advantage of high diffraction efficiency, but they present both chromatic selectivity and chromatic dispersion, which impact their use with wide spectrum light sources. Single-color light emitting diode (LED) sources have a narrow spectrum that reduces these issues and this makes them better suited for use with volume HOEs. However, the LED source size must be taken into consideration for compact volume HOE-LED systems. To investigate the design limits for compact HOE-LED systems, a theoretical and experimental study was carried out on the effects of an extended source on the HOE output for different holographic lenses, with focal lengths from 25-100 mm. The lenses were recorded in a commercially available photopolymer [Bayfol HX200], and their diffraction efficiency was characterized across the lens aperture by measuring the Bragg angular selectivity curve at each location. Offset point sources were used to experimentally study the effects of a non-point source on the HOEs, and the system was modeled using Matlab and Zemax.

Keywords: holographic optical element; LED; Bragg selectivity; holography; diffraction

Paper 23035G received Oct. 13, 2023; revised Jan. 5, 2024; accepted Jan. 9, 2024; published Feb. 14, 2024.

1 Introduction

Applications of volume holography and holographic devices/holographic optical elements (HOEs) research have increased significantly in the last decade due to advances in materials,[1] devices,[2] and their mass manufacture techniques.[3,4] The combination of the lightweight and low-cost format, paired with the flexible design, gives them the potential to replace conventional optics with more compact, versatile designs. Nevertheless, many challenges remain, and using diffractive devices with spectrally broad sources, such as solar and light emitting diode (LED) light, requires further innovation to counteract dispersion and angular and wavelength selectivity issues.[5] Single-color LEDs have a relatively narrow spectral bandwidth and are available in low-cost, flexible formats that also suit compact optical systems. LEDs, despite these advantages, introduce their own challenges for HOE devices. The light output cone angle is very large,

*Address all correspondence to Suzanne Martin, suzanne.martin@tudublin.ie

sometimes 120 degrees, the output light is unpolarized, and it emanates from a surface that has a significant surface area. This can cause difficulties collecting light at the HOE and matching the HOE microstructure to the collected light for maximum Bragg diffraction, presenting challenges in ensuring high efficiency and low aberrations. In different applications and optical arrangements, different aspects of these challenges dominate, but in most cases, the size of an LED source must be taken into consideration, and this becomes increasingly significant the more compact the system is. In this paper, which was previously published as a conference paper,[6] the issues that arise as a result of the finite area of the light source are investigated, and the limitations that this imposes on the LED-HOE system design are discussed.

2 Theoretical Background

Diffractive optical elements (DOEs) redirect light using diffraction instead of refraction or reflection and achieve similar results to common optics but in a very thin, flexible, and compact format, which makes them very appealing for different uses.[7] Within the broader category of DOEs, HOEs are those that are created by recording interference patterns into suitable materials. Depending on the relationship between the spatial period of the recorded pattern and the thickness of the material, they can be either volume HOEs[8] or thin holographic elements. Volume HOEs benefit from higher diffraction efficiency because, instead of diffracting light into multiple orders, they re-direct light into a single order.

The simplest HOEs are gratings,[9] meaning they have the same spatial frequency throughout the whole HOE. These can be made by recording the interference of two collimated beams. The incident angle (with respect to the fringe planes) at which maximum diffraction efficiency occurs is called the Bragg angle (θ_B) and is expressed in the following equation:

$$\lambda = 2 \cdot n \cdot \Lambda \cdot \sin\theta_B, \tag{1}$$

where λ is the reconstruction wavelength (θ_B (inside the material) will be different for each λ), Λ is the spatial period, and n is the refractive index of the medium.

Figure 1 shows the general relationship between the recording and reconstruction beams and the recorded grating. k_r and k_o represent the modulus of the wavevector of the reference beam and object beam during recording, respectively; k_p and k_d represent the modulus of the wavevector of the incident and diffracted beam during replay, respectively; and K represents the modulus of the grating vector.

For a grating being probed at the same wavelength at which it was recorded, the Bragg condition is met when $\theta_r - \theta_p = 0$, meaning that there is no difference in angle between the recording angle and the probing angle.

For volume phase gratings, the refractive index is modulated during recording to produce a sinusoidal pattern.[10]

If the volume grating is a phase only, that is, the interference pattern is recorded in the material as refractive index or thickness changes, the efficiency of the diffracted beam can reach

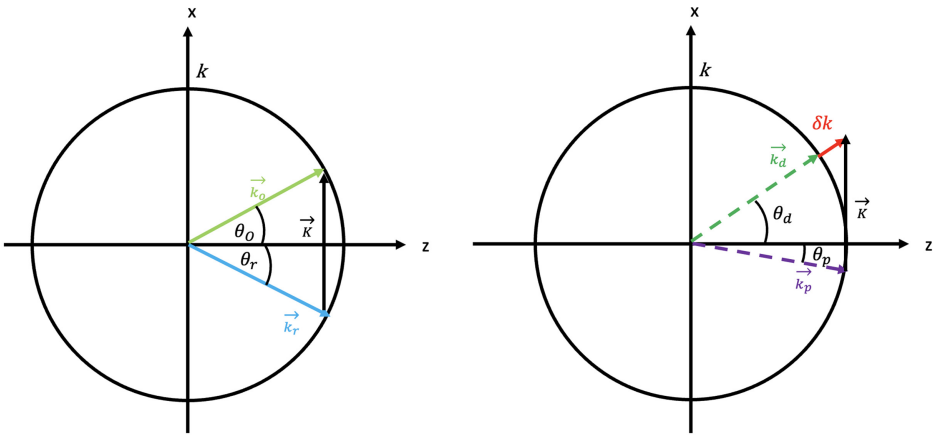

Fig. 1 Schematic showing wave vectors k_r, k_o, k_p, k_d, K, and δk as well as the corresponding angles θ_r, θ_o, θ_p, and θ_d.

100%. In this case, the diffraction efficiency of the output is given by Eq. (2), which is an approximation from Kogelnik coupled wave theory (KCWT):[11]

$$\eta = \left[\frac{\sin\sqrt{\xi^2 + v^2}}{\sqrt{1 + \frac{\xi^2}{v^2}}}\right]^2. \tag{2}$$

In Eq. (3), ν is the phase parameter, which is directly associated with the modulation index obtained within the material and is expressed by the following formula, where θ_d is the diffracted angle and θ_p the probing angle (both angles inside the material):

$$\nu = \frac{\pi n_1 T}{\lambda\sqrt{\cos\theta_d \cos\theta_p}}, \tag{3}$$

and the angular detuning parameter is given by ξ as[12]

$$\xi = \frac{\Delta\theta \cdot 2 \cdot \pi \cdot n \cdot T \cdot \sin\theta_B}{\lambda}. \tag{4}$$

For a phase grating, this allows for calculations of the DE (η) at a range of angle mismatches $\Delta\theta$ from the Bragg angle. T is the thickness, n_1 is the average refractive index of the layer, θ_B the Bragg angle, and λ the reconstruction wavelength. If the illumination angle deviates from the Bragg value ($\Delta\theta$ increases), the efficiency of the grating decreases. The slant of the planes of equal refractive index generated inside the grating, together with the spatial period, determine the direction of the diffracted rays.

If one of the beams interfering at the recording is a divergent beam instead of a plane one, the holographic element is not a grating but a holographic lens.[13] In this case, the slant and the period of the refractive index variations are not constant along the hologram. A holographic lens can divert 100% of a divergent input beam into a collimated beam at the output as long as the Bragg condition is met everywhere, i.e., as long as the input beam exactly matches the incident beam for which the HOE was designed.

In real applications, several challenges arise in meeting this criterion, the first being the non-zero range of wavelengths in any real light source. Chromatic aberrations in holographic systems are well understood[14] and, of course, cause few issues when working with laser sources. However, for applications with LED sources (the main topic of interest here), the variation of Bragg angle with wavelength produces significant dispersion. Holographic lenses form a different focal distance for each wavelength, and if the HOE is an off-axis element, as is commonly the case, the plane waves at the output have different directions for each wavelength. In single color LED systems, the issue is reduced but not eliminated. Research into methods to minimize this is the topic of other studies.[15] The second issue is the fact that, for perfect Bragg matching at all points across the HOE, a perfect point source is needed. This is a particular challenge for LEDs, which usually consist of a square or rectangular emitting surface of millimeter dimensions. In addition, the highly diverging output from a LED source requires a high numerical aperture HOE lens, usually positioned quite close to the source. HOE lenses for LED applications are typically holographically recorded by interfering a collimated beam and a divergent beam, so the HOE lens is suitable for a divergent source at the reconstruction stage that would provide a collimated beam as an output. Such an arrangement is shown in Fig. 2.

For such an HOE, it is clear that the photonic structure can vary considerably across its aperture in terms of both spatial frequency and slant. It is also worth noting that such lenses are usually designed to be off-axis to avoid very low spatial frequency areas that would not meet the criteria for the volume regime and would therefore diffract multiple beams.

To investigate worst-case constraints introduced by source size on a functional volume HOE lens, we calculate the mismatch caused at the HOE by an offset in the source position on the LED. Figure 3 is a schematic that represents the rays arriving at the HOE from different parts of the LED source. The extreme rays emanating from the ends of a LED and the central ray, along with the resulting angular mismatch that results as those rays reach the plane of the HOE lens, are shown. The angular difference ($\theta_{OB} \pm \theta_{Offset}$) represents the range of rays that will be incident at a particular point on the HOE as a result of the size of the LED. This will vary depending on the distance of the source from the HOE, with smaller discrepancies observed at greater distances.

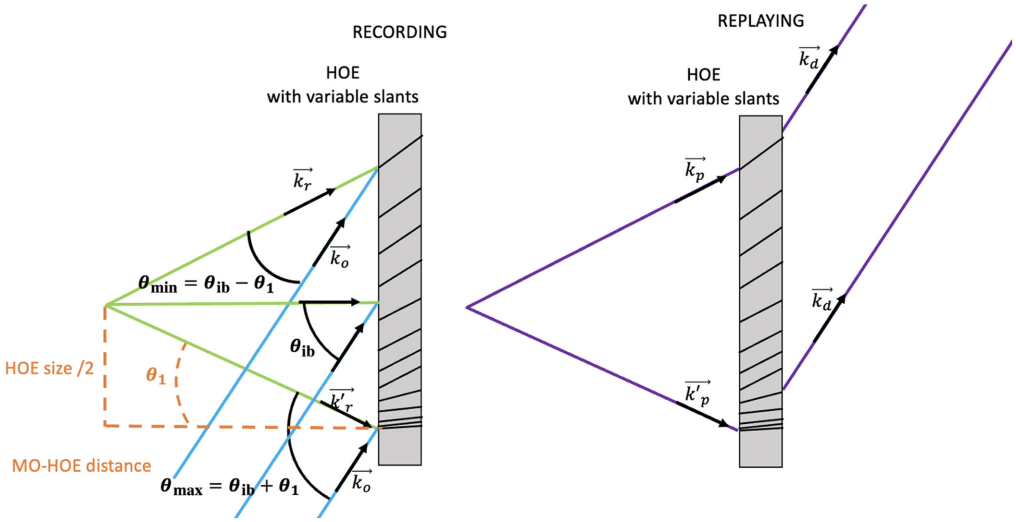

Fig. 2 Schematic showing recording with a diverging beam and a collimated beam (left), and replaying (right.) θ_{ib} is the central interbeam angle and θ_1 is the aperture angle.

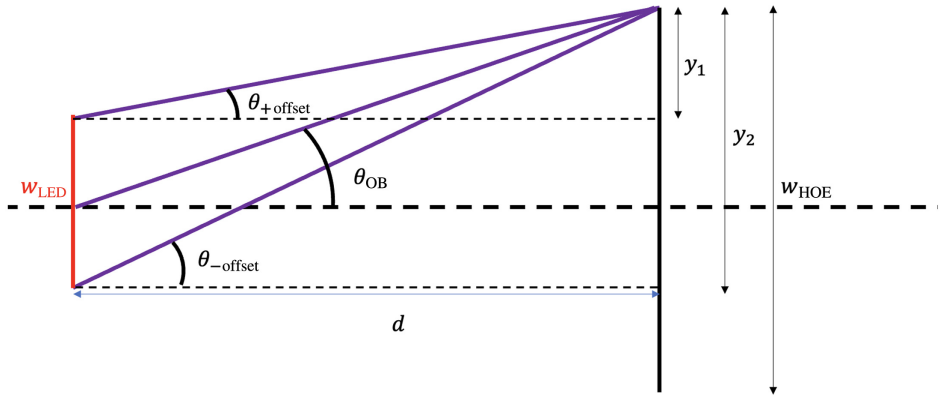

Fig. 3 Schematic of the angular mismatch $\theta_{+offset}$ and $\theta_{-offset}$ introduced by the size of the LED source, showing rays emanating from the extreme ends of an LED reaching the same point on an HOE. The central ray is depicted as θ_{OB} being the on Bragg ray. y_1 and y_2 are the distances used to calculate the two offset angles and then the angular mismatch from Bragg angle at this particular point of the HOE, respectively.

Because we are assessing only the "worst case" at the LED edge, this is not expected to allow for an exact model of the energy distribution in an LED's output beam, but rather an indication of the limits at which the size of the source becomes a problem and begins to significantly influence the performance of the HOE.

As we show below, the deviation from the "perfect" angle of incidence from the light arriving at the HOE has two effects on the output: (1) the incoming light will be off Bragg and as such will cause reduced efficiency and therefore lower intensity in the output light; (2) diffracted light will deviate from the design angle.

In any volume hologram, the intensity of the diffracted beam is dependent on the reconstruction angle and the incident beam should match the Bragg angle (assuming no change in wavelength) to achieve the theoretical maximum efficiency of 100%. When the angle of incidence does not match the Bragg condition for the grating at any location, the diffraction efficiency is lowered and the intensity in the output beam is reduced. This well understood effect is often referred to as "Bragg selectivity" and can be modeled by plotting the diffraction efficiency as a function of the angular offset from the Bragg angle for a given thickness, spatial frequency, wavelength, angle, and material refractive index using Eq. (2).

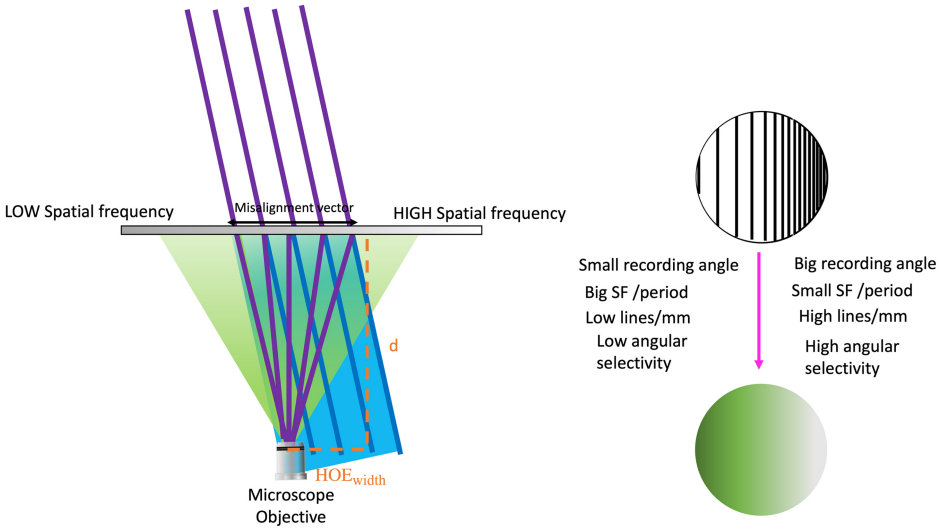

Fig. 4 Schematic showing the replaying of the HOE lens with a diverging source on the left and schematics depicting the expected spatial frequency variation across the HOE and the expected intensity variation across the output beam as a result of an offset position on the right. The distance *d* varies in the range of 25 to 100 mm.

Table 1 Table showing the values of the maximum and minimum theoretical spatial frequencies for each recorded HOL distance with a total surface of 12 mm and a central angles of 23.9 deg.

Light source - HOE distance (mm)	SF (min) (ln/mm)	SF (max) (ln/mm)
25	340	1205
40	502	1050
70	620	934
100	667	888

In an HOE lens, the spatial frequency varies, resulting in a different Bragg selectivity at different locations across the lens. As a consequence, the change in diffraction efficiency across the lens will not be uniform, even if there were a uniform angular change (which is not the case). To predict the response of the local diffraction efficiency to a change in angle of incidence, the knowledge of the local spatial frequency is essential. Figure 4 depicts how the variation in spatial frequency across the HOE lens causes an asymmetrical reduction in the intensity of the diffracted beam when the hologram is illuminated with a point source offset on the horizontal plane. In Fig. 4, we can observe the two recording beams (divergent purple rays) and a collimated reconstructed beam (parallel purple rays) exiting the hologram. The left side of the lens has lower spatial frequency (low angular selectivity) than the right part (high angular selectivity) in Fig. 4. As we can see on Table 1, depending on the distance at which the HOL is recorded, for the same width of recording and central beam angle, the obtained spatial frequencies vary widely as explained above.

3 Materials and Methods

3.1 Photosensitive Material

Bayfol HX®[16] was used for the holographic recording. This is a well-known material, sensitive to a wide range of wavelengths between 400 and 700 nm.[10] Composed of three layers, substrate, photopolymer layer of 16 μm and protective film, it can be laminated onto a rigid substrate to give the layer the stability required when recording the holograms. The refractive index

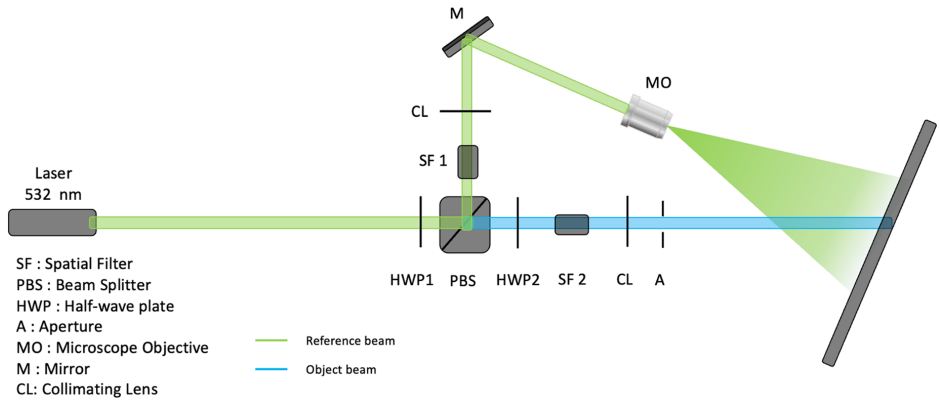

Fig. 5 Diagram of the recording setup.

modulation (n_1) of the photomaterial depends on the spatial frequency (Λ), but it can be around 0.025, which is more than enough, with a 16 μm thickness, to give 100% efficiency for a wavelength of around 532 nm.

3.2 Recording Setup

The four holographic lenses simulated in Sec. 3.3 were recorded experimentally in Bayfol HX200. Figure 5 is a schematic of the recording arrangement used. The setup consists of a Verdi laser from Coherent Inc., which is split and sent into two spatial filters and collimating lenses to provide two collimated beams. The intensity ratio of the two recording beams is controlled using a polarizing beam splitter and two half-wave plates (PBS, HWP1, and HWP2). The first beam has an aperture and remains collimated, whereas the second beam is reflected via a mirror directly onto a microscope objective 20× (MO) to create a narrow focal point, so it then propagates with very high divergence. The inter beam angle between these two will be 23.90 deg. The MO is mounted onto a custom-printed slider to allow for movement along the z-axis for the different distance recording.

The recording of the samples was achieved with a 0.3 W laser intensity of input for all of the samples. The equalizing of beams was achieved by adjusting the HWP before the beam splitter (BS), and the different times of exposure were calculated with the 10 mJ/cm^2 to achieve nearly 100% diffraction efficiency.[10] The recording intensities for both beams as well as the recording times are shown in Table 2 for the different distances from the MO to the sample.

3.3 Modeling

3.3.1 *Matlab modeling*

Matlab® was used to develop multiple individual scripts that allowed us to both calculate and model a number of things: (a) the microstructure of the HOE (based on the recording setup, wavelength, and characteristics of the recording material), (b) the resulting local Bragg selectivity, (c) the expected angular offset from Bragg at the HOE due to a given source misalignment (assumed to be analogous to the source size in an LED), and (d) the expected local diffraction efficiency due to the selectivity modeled in (b) and the off-Bragg angle expected from (c).

Table 2 Table showing the values used for the recorded samples. Irradiance measured at the plane of recording.

Light source - HOE distance (mm)	Irradiance of divergent beam (μW/cm^2)	Irradiance of collimated beam (μW/cm^2)	Exposure time (s)
100	45	44.3	112
70	76	74.5	66
40	161.3	165.1	31
25	284.2	285.2	17

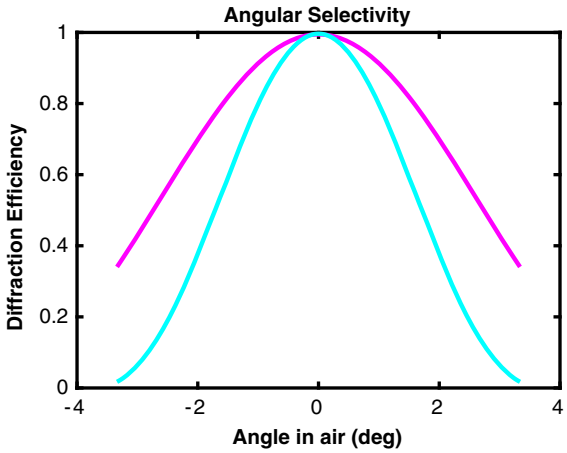

Fig. 6 Graph showing the calculated angular selectivity plot at the −10 mm (pink line) and the +10 mm (cyan line) positions for a 20 mm HOE recorded at a 100 mm distance.

We consider four holographic lenses with different numerical apertures: 0.4, 0.25,0.14, and 0.1. These are created by arranging different distances from the divergent source to the holographic material during the holographic recording (25, 40, 70, and 100 mm), while keeping width of the recorded HOE constant at 20 mm. The central interbeam angle in the recording step was 23.90 deg for the four lenses. With this information, the local slant and spatial frequency were calculated across the HOE. Knowing the spatial frequency at each point of the HOE allows for calculation of angular selectivity at each point of the lens [Eqs. (2)–(4)]. Refraction at the air-glass boundary is taken into account, so the values calculated are inside the recording medium.

Figure 6 shows a plot of diffraction efficiency versus angular deviation from the Bragg obtained for the ±10 mm positions on the 20 mm HOE and is a typical example of the calculated plots, which allow us to assign a diffraction efficiency value for every angular deviation from the Bragg angle. It is important to note that this curve is unique for each point across the HOE lens due to the difference in local spatial frequency.

The difference between the incident angles ($\theta_{+\text{offset}}$ and $\theta_{-\text{offset}}$) and the θ_{OB} is calculated as described in Sec. 2, which for each location on the HOE gave a value for the expected magnitude of the deviation of the actual angle of incidence from the Bragg angle of incidence at that location. This allows the angular mismatch from Bragg to be calculated as a function of position on the HOE for the four lenses and for different source transversal positions. Next, a script was created to calculate the theoretical diffraction efficiency across the element. To achieve this spatial frequencies and slants already calculated at each location on the HOE are used with Eqs. (2)–(4) to calculate the local diffraction efficiency at that point on the HOE.

Knowing the angular mismatch from Bragg as a function of position on the HOE, and with the help of Eqs. (2)–(4) for every point on the HOE, it is now possible to calculate and plot the diffraction efficiency across the HOE for the four lenses when the point source is displaced (i.e., considering an extended source at reconstruction). Because this calculation uses Kogelnik coupled wave theory,[11] it is important to note that all parts of the HOE should be in the volume grating regime.

3.3.2 *Zemax modeling*

The four holographic lenses were simulated in ray tracing software (Zemax). Each holographic lens was defined using the specific recording beams outlined in Fig. 2. Zemax was then used to model the output to take into account the effect of the source size, and ray tracing is simulated from five divergent point source positions. One point source is on axis, and the other four are shifted.

A similar model was generated for each of the four source-HOE distances in sequential mode to allow for the automatic calculation and conversion into non sequential mode, to use ray tracing to obtain a readout of the intensity on a detector placed at a certain distance.

3.4 Testing

Two different texting methods were used to experimentally explore the effect of an extended or offset source on the diffracted beam.

3.4.1 *Output beam analysis at a range of offsets in the source position*

Because a light source that has an extended emitting surface can be thought of as a series of laterally displaced point sources, it should be possible to better understand the effect of having a source with a specific size, by examining the behavior of a point source that has been displaced by a distance similar to the LED size. In the approach used here, the HOE is illuminated with a diverging laser beam equal to that used in recording but much larger than the HOE. This beam emulates the light coming from a point on the surface of the LED. A camera was placed on the same axis as the slide holder and at the same height to capture a video as close to the central position of the holographic lens as possible. During the experiment, the HOE lens holder was moved (introducing a relative shift in the source position relative to the HOE) first to the right and then to the left, stopping at ± 3 mm $\pm$ 6 mm positions for 3 s for later gathering and processing of the frames, which is discussed later. Figure 7 shows a sketch of the arrangement, showing the "probe" beam diverging from the microscope objective and the arrangement of the camera capturing images of the diffracted beam.

The images were captured using an iPhone camera attached to a 3D printed holder, placed directly next to the sample holder on the same horizontal axis and parallel to the screen. The samples were illuminated with the appropriate object beam to reconstruct the collimated beam as output, for the distances required by each sample. Due to the high intensity of the beam and with the aim of avoiding over-exposure in the image, the ISO (camera's sensitivity to light) was lowered to keep the results consistent as the video was captured, with a fixed ISO, while samples were moved laterally in the horizontal plane to positions ± 3 mm and ± 6 mm. The next step was to extract the frames corresponding to each desired illumination offset for all of the samples, so they could be inputted into ImageJ to evaluate the intensity change across the image.

A 390 px long line was drawn across the image of the diffracted output for each sample to retrieve the gray level values per pixel and allow for further processing in Matlab.

Figure 8 depicts the setup used for the probing to obtain the angular selectivity curves from which we measured the angles of maximum diffraction to calculate the slant angle and the spatial period, given in Fig. 10.

3.4.2 *Testing with an LED source*

For this test, the HOE was illuminated using an LED. An LED was placed in a custom PCB with a 3D-printed base attached to the same carriage that the MO used in recording.

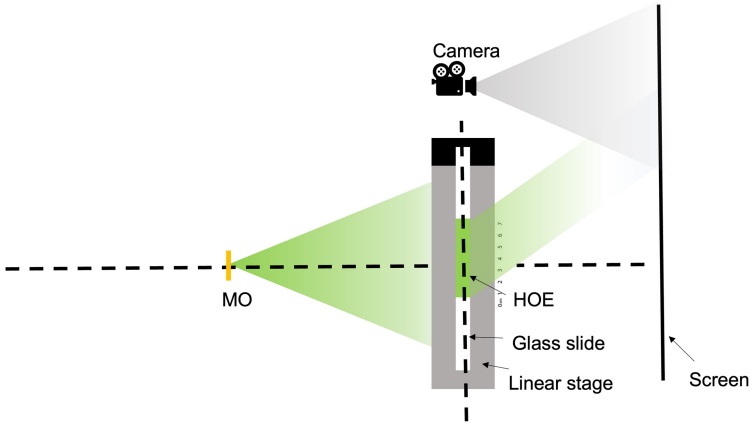

Fig. 7 Diagram of the setup for the output beam analysis of offsets in the source position.

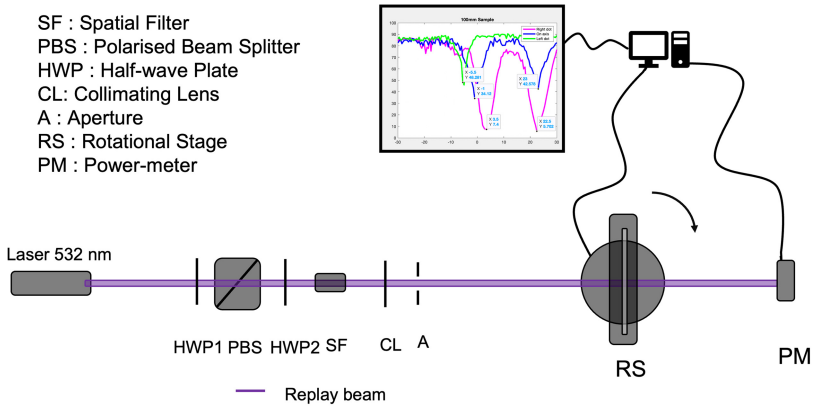

Fig. 8 Diagram of the probing setup for the gathering of the angular selectivity curves from the four HOE lenses.

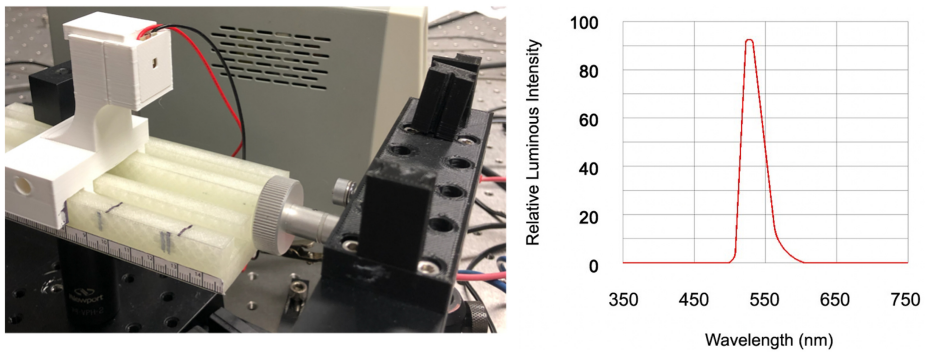

Fig. 9 Image of the LED mounted on top of the setup that ensures alignment (3D printed part) (a) and relative intensity versus wavelength of the LED[17] (b).

The HOEs were also placed on it, so it would reproduce as closely as possible the characteristics of the recording beam with which the samples were generated. The LED was a PLCC2 SMD (SMS 1105PGC) with a dominant wave of 532 nm with an emitting angle of 120 deg and a wavelength bandwidth, as shown in Fig. 9. After adjusting the HOE to be approximately on-Bragg (normal incidence of the principle ray from the LED on the center of the HOE), the diffracted beam output produced was arranged so it fell on a screen arranged parallel to the planes of the holographic lens at a 150 mm distance where the resulting illumination pattern was photographed.

4 Results and Discussion

4.1 HOE Lens Probing and Testing

The recorded HOE lenses were tested to ensure that the expected structure was recorded by measuring their angular selectivity curves (Bragg curves) locally across the element.

Figure 10 shows slant and grating periods calculated directly from local Bragg curve peak positions, alongside modeled values expected across the aperture of the HOE lens. Though agreement is not perfect across all samples, this confirms that the micro-structure of the recorded HOE lenses matched the expected micro-structure to <1 deg.

The error is most likely due to the large (0.5 deg) step used when probing, which gives the Bragg curves and therefore the values used to calculate the experimentally obtained slant and period as seen in Fig. 8. Therefore, an uncertainty of 0.25 deg for the slant and $0.05 \cdot 10^{-6}$ m was introduced and is shown in Fig. 10 as the error bar.

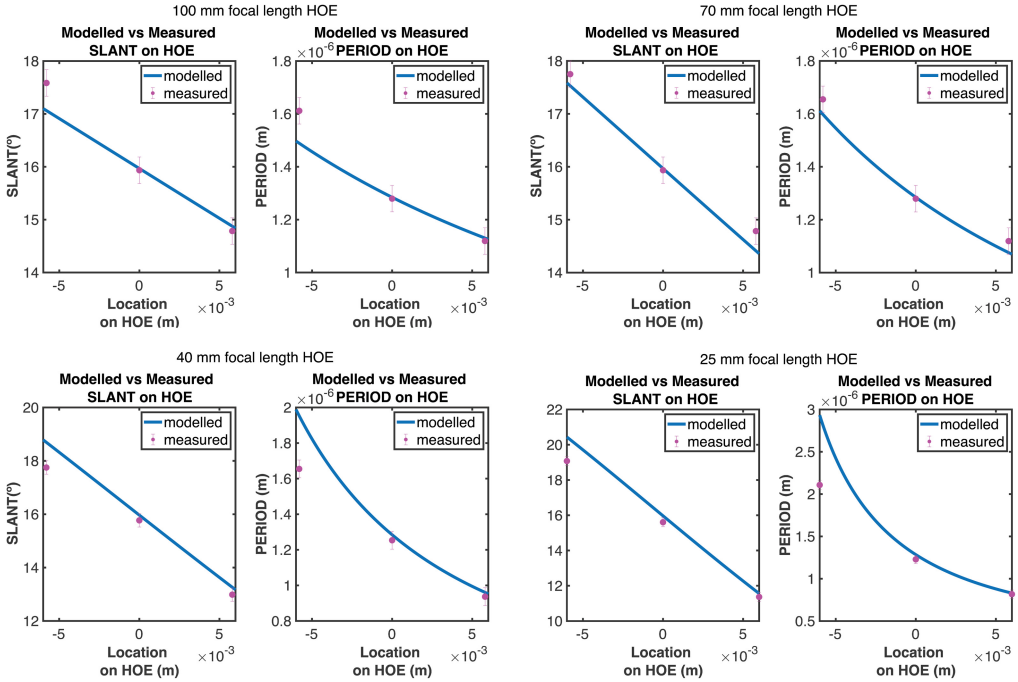

Fig. 10 Graphs comparing slant and spatial period as a function of location on the HOE lens for all four HOE lenses.

4.2 Study of the Effect of Source Offset on Diffraction Efficiency using MATLAB Modeling

As described in more detail in the methods section above, a Matlab model was then developed to calculate the angular mismatch, as seen in Fig. 3, that would be expected at the HOE lens. This of course depends on source position/offset and the distance between the HOE and the source, as well as the position on the HOE or more specifically the distance from the center of the HOE lens.

Knowing the angular deviation/mismatch at each location and also the grating spatial frequency, the effect of the mismatch on diffraction efficiency can be calculated. Figure 11 shows the model results for the expected diffraction efficiency as a result of that Bragg mismatch at any particular location on the HOE.

Each panel in Fig. 11 shows the expected diffraction efficiency of the HOEs diffractive structure as a function of location on the HOE, based on knowledge of the locally modeled Bragg selectivity and the illumination angles deviation from the ideal at that location.

The diffraction efficiency was modeled in Matlab for the four source-HOE distances and for five points across the surface (+6 mm, +3 mm, 0 mm, −3 mm, and −6 mm). The on-axis point shows no decrease in diffraction efficiency as the misalignment is zero, so the rays match the perfect on-Bragg incidence angle at every location; this gives a theoretical 100% efficiency throughout the full aperture of the HOE. As the source is moved to an offset position, the angle of incidence at each position on the HOE changes, and a reduced diffraction efficiency is observed. The diffraction efficiency decreases as the offset is increased, indicating the reduced intensity in the diffracted beam that could be expected for these source position offset values.

The main observations from the Matlab model predictions are as follows:

1. The model assumes 100% efficiency across the whole lens when the source is perfectly on axis.
2. In all cases, it is observed that the left side of the graph, which corresponds to the lower spatial frequency region, has higher efficiency. This is due to the lower angular selectivity that occurs at lower spatial frequencies—any angular mismatch caused at the HOE has less of an effect.
3. The overall efficiency of the HOE lens decreases with the HOE lens focal length (increasing numerical aperture) and increasing source offset.

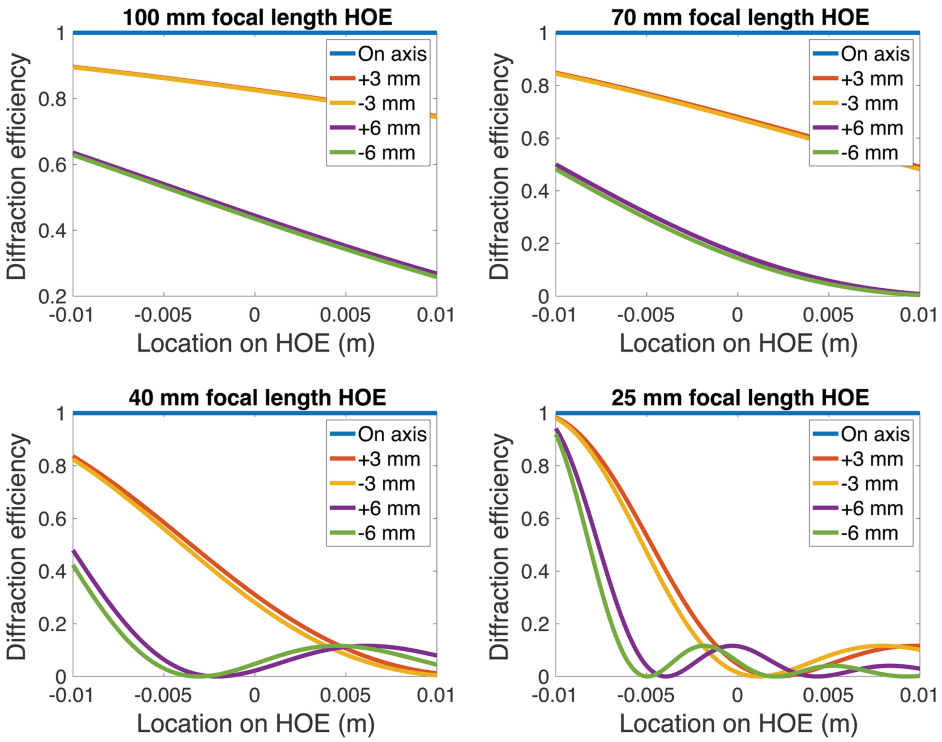

Fig. 11 Graph showing the modeled diffraction efficiency for 0, ±3, and ±6 mm source offsets for four HOE lens samples.

This Matlab model takes local angular selectivity into account but does not yet account for aberrations. For that reason, Zemax was used to understand the role of aberrations in the output beam.

4.3 Experimental Study of the Effect of a Misaligned Source on the Output of the HOE Lens

Next, the four HOE lenses were tested with a diverging laser beam that, when on axis, was optimally matched to the HOE lens design (i.e., it was one of the recording beams). Then, a series of lateral offsets were introduced in the source position, so the effect on the diffracted output beam could be assessed. Figure 12 shows images of the output diffracted beam for four HOE lenses as the offset of the source from its ideal on-axis position is varied. This is helpful in visualizing the effects of a non-centered source. It should be noted that the lateral shift of the output beam was not measured in this experiment—only the relative intensity distribution within the output beam is studied here.

We can make a number of observations from this experimental data. (1) The shorter the focal length is, the lower the tolerance to an offset source position is. We see a trend of overall efficiency decreasing with increasing source offset in line with Matlab predictions. (2) In all HOE lenses, there appears to be a general tendency for the right side to retain higher intensity as the offset is increased. This general trend is also in line with the Matlab prediction. (3) This tendency appears to be greater as the focal length decreases, but it is difficult to compare across lenses because of variations in the baseline intensity and local variations in diffraction efficiency that are visible even on axis. See below for further analysis using ImageJ. (4) All of the samples share a more pronounced reduction in diffraction efficiency for the positive mismatch than the negative ones—this has the same trend as the predictions in the Matlab model. (5) The depicted maximum intensity of the samples cannot be compared across the different set of samples due to the difference of recording distance. Replaying with the same source, but from different distances, causes a change in the intensity at the HOE. It is also important to note that the diffraction efficiency in the column that represents the on-axis source is not uniform and not 100% as is the case in the Matlab model. This is due to variations in the uniformity of intensity in exposure step and

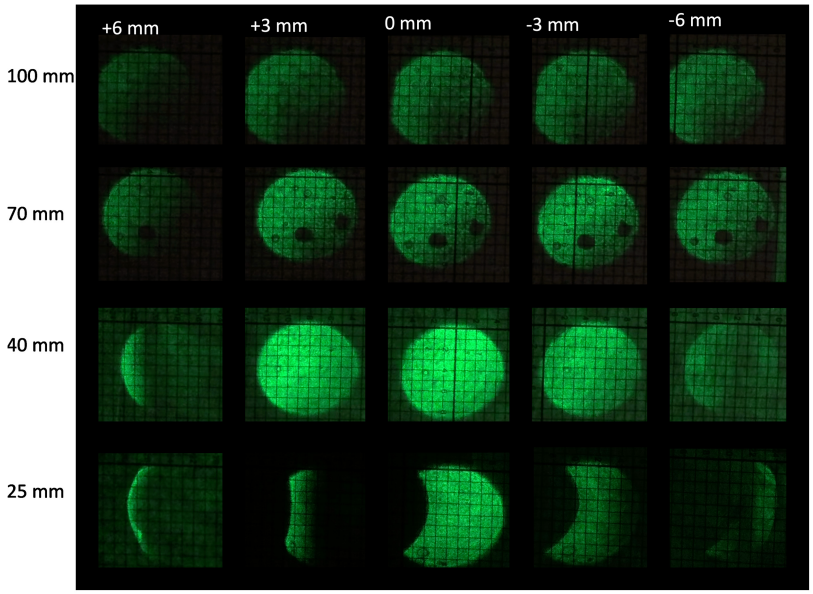

Fig. 12 Images gathered from the diffracted beam for the four holographic lenses with a range of different misalignments of the illuminating point source. The source to HOE distance for each row is shown on the left, and the distance from the axis at which the source was positioned is indicated on top in mm. The screen was positioned 150 mm away from the HOE for all images. Some artifacts can be observed on the 70 mm sample under the shape of three circular bubbles.

the different divergence in the recording beam for each HOE, a common problem in HOE recording.[12,18] Note also that the missing part of the surface in the 25 mm sample is due to an impingement between the microscope objective used to provide the diverging recording beam and the collimated beam during recording, and there is an artifact showing on the 70 mm sample in the form of three circular bubbles.

4.4 IMAGEJ Analysis of Experimental Data

The images in Fig. 13 show the distribution of intensity across the approximate horizontal center of the output (diffracted) beam from the HOE lenses. They were obtained using ImageJ from the images in Fig. 12. Manual selection of the appropriate area was necessary because the changing diffraction angle meant that the output beam moved laterally across the screen, making it impossible to set a common (0,0). The background of the images under analysis contains grid lines, so a moving mean was used for each individual data set. When comparing with Matlab model results, note that, even when completely "on Bragg" at the central source position, the intensity of the diffracted beam is not uniform across the HOE. This is due to a combination of the Gaussian recording beam, imperfections in the lamination process, and a non-uniform recording process. The dark blue curve in Fig. 13 represents the maximum diffraction efficiency obtained in that particular HOE lens.

4.5 Zemax Modeling Results

To better understand the images obtained above, especially at shorter focal lengths, a Zemax model was created for the HOE lenses and reconstructed with sources that are offset by distances equal to those used in the above experiments. The images on Fig. 14 show the results for the predicted output beam at the same distance from the HOE as the screen in the experimental data. False color is used to compare the diffracted beam intensity with the different offsets. Intensity bars are not shown because the input power intensity is an arbitrary 1 W, which is represented by the bar showing red as the maximum irradiance and blue as the minimum.

The Zemax results add significant information, primarily because aberrations are taken into account. The model results for the longer focal length HOE lenses show the same left to right diffraction efficiency dependence as seen in the model and data above, but the significant changes in the beam shape seen in the experimental data for the shorter focal length lenses are also visible.

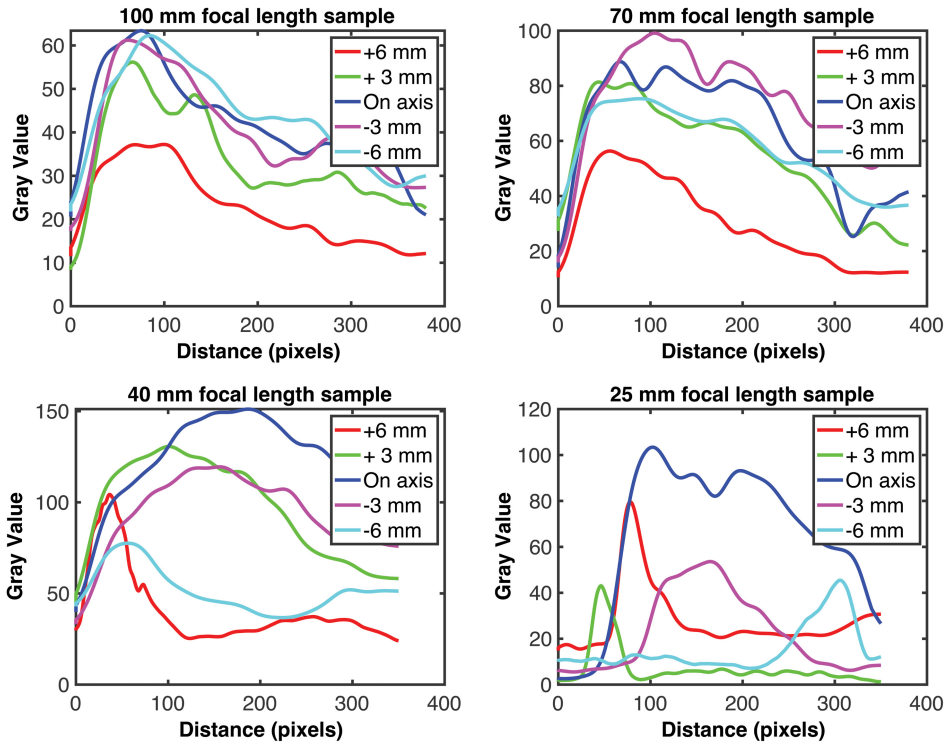

Fig. 13 Graph showing the trends obtained from a moving average treatment of ImageJ data from Fig. 12 for each of the four HOE lenses.

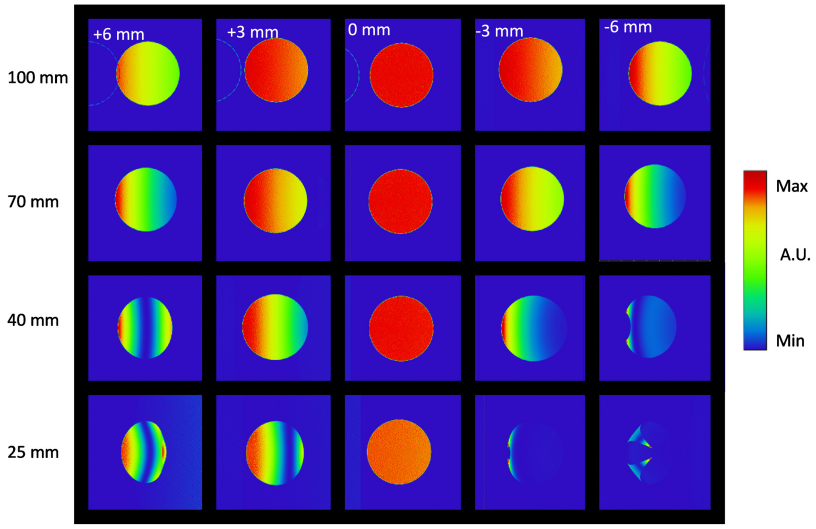

Fig. 14 Images from the Zemax model, at a 150 mm distance from the HOE, for each HOE lens at a range of different source misalignments. The source to HOE distance for each row is shown on the left, and the distance from the axis at which the source was positioned is indicated on top in mm. The screen was positioned 150 mm away from the HOE for all images.

4.6 LED Reconstruction

The images in Fig. 15 show the diffracted beam for the four lenses when illuminated with a narrow-band green LED source.

The images from Fig. 15 are captured at a screen set at the same distance from the HOE as the screen in the images in Fig. 12 (150 mm). Evidence of the features discussed above is visible. The images are shown in black-and-white, so the distracting spectral variation is not visible, as

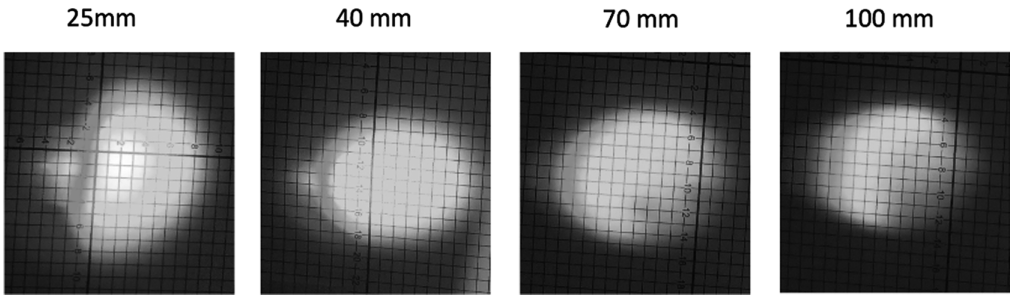

Fig. 15 Graph showing the obtained output from the samples when reconstructed with an LED (BW filter was applied).

chromatic aberration is not under study here. Although the model above is deliberately extended to quite significant offsets, commonly used LEDs are usually not larger than 3 mm. This particular LED is 1.8 mm in diameter, so the worst-case "source position" at its edges offset lies between the ± 3 mm results shown in Fig. 11. Figure 15 shows the output obtained when the four HOLs in this study are used to re-direct light from a typical green LED. In each case, the HOL redirected the light to the desired angle, approximately following the behavior that the presented models had predicted. Note that, when a HOL is used with a real LED, an output (diffracted beam) equivalent to the sum of the predicted outputs at a range of point-source offsets is expected, due to the extended LED emitting surface. In this initial trial, it was observed that for the HOLs with shorter distances between the HOL and LED source, larger aberrations are apparent in the output beam and there was a general trend for more intensity to the left side of the beams, as observed in the modeling above. Discreet bands of off-Bragg and on-Bragg sections were not as visible with the real LED sources, however, presumably because of an averaging effect.

5 Conclusion

The limits for misalignment of source position have been explored for a set of HOE lenses in the context of modeling the effects of the extended nature of LED sources. Four HOE lenses were successfully holographically recorded using Bayfol HX200, and their structure was confirmed using Bragg analysis. The HOE lenses had focal lengths 100, 70, 40, and 25 mm and were designed to accept an on-axis diverging beam and produce an off-axis collimated beam with a diameter of 20 mm. The HOE lenses were probed with diverging laser light, which was displaced laterally from the original position to mimic light coming from the extreme edge of LEDs of different sizes, aligning the source first on-axis (maximum Bragg match) and then at a range of offset source positions. The diffracted beam intensity profile was captured using a video camera and analyzed using ImageJ.

A Matlab model was developed; it took into account of the angular mismatch at the HOE as a result of the offset source position, as well as the range of spatial frequencies across the lens. The output of the Matlab model was a dependence of diffraction efficiency on position across the HOE, calculated for different offsets in the source position. A Zemax model was also used to model the system. The Zemax analysis also took into account the source offset and local spatial frequency, as above, but it also included aberrations.

The experimental data demonstrated that the intensity and uniformity of the HOE's output decreased with increasing offset in the source position. In addition, it was observed that this effect became more severe as the focal length of the HOE decreased. Both models also showed these trends. For the largest source offsets and shortest HOE focal lengths, we begin to see dips in the Matlab graphs, which approximately correspond to the vertical "fringe" visible in the experimental images and the minima in the Zemax false color images. Overall, good agreement is obtained for the experimental results and both models. However, the Zemax predictions are better matched for the 25 mm focal length HOE lens, most probably due to the fact that the Matlab model developed here does not yet take aberrations into account.

This work is a first step in developing a simple modeling approach that allows designers of systems using HOEs with LED sources to quickly determine the source-size limits for specific HOE-LED distances. Further work will involve testing the model with LED sources of different source dimensions at a range of distances and incorporating the local change in beam direction that accompanies an off-Bragg incident beam into the Matlab model.

Acknowledgments

This publication has emanated from research conducted with the financial support of Science Foundation Ireland (Grant No. 20/FFP-P/8851). The authors thank FOCAS, TU Dublin, for the technical facilities and administrative support provided.

Code and Data Availability

The data used in this paper as well as the pieces of code referred in it have been uploaded and can be accessed at the recommended platform by SPIE named Code Ocean.

Link: https://doi.org/10.24433/CO.4650848.v1

Script 1 holds the calculations described initially in 2 as well as the modeling shown in 3.3.

Script 2 shows the calculations represented in 3 for the error in angle committed depending on certain dimension values.

Script 3 was used to obtain images shown in 13.

Script 4 was used to obtain images shown in 10.

Script 5 was used to obtain images shown in 11.

References

1. B. Rogers et al., "Improving the holographic recording characteristics of a water-resistant photosensitive sol–gel for use in volume holographic optical elements," *Photonics* **9**(9), 636 (2022).
2. P.-A. Blanche, A. H. Mahamat, and E. Buoye, "Thermal properties of Bayfol® HX200 photopolymer," *Materials* **13**(23), 5498 (2020).
3. D. Vather et al., "Serialized holography for brand protection and authentication," *Appl. Opt.* **57**(22), E131–E137 (2018).
4. F.-K. Bruder, T. Fäcke, and T. Rölle, "The chemistry and physics of Bayfol® HX film holographic photopolymer," *Polymers* **9**(12), 472 (2017).
5. S. Keshri et al., "Stacked volume holographic gratings for extending the operational wavelength range in led and solar applications," *Appl. Opt.* **59**(8), 2569–2579 (2020).
6. J. Lasarte et al., "Modelling HOE performance with an extended source: experimental investigation using misaligned point sources," *Proc. SPIE* **12574**, 1257405 (2023).
7. J. Xiong et al., "Holographic optical elements for augmented reality: principles, present status, and future perspectives," *Adv. Photonics Res.* **2**(1), 2000049 (2021).
8. C.-C. Sun and P. P. Banerjee, "Volume holographic optical elements," *Opt. Eng.* **43**(9), 1957–1958 (2004).
9. N. Kim, Y.-L. Piao, and H.-Y. Wu, "Holographic optical elements and application," *Holograph. Mater. Opt. Syst.* **5**, 99–131 (2017).
10. J. Marín-Sáez et al., "Characterization of volume holographic optical elements recorded in Bayfol hx photopolymer for solar photovoltaic applications," *Opt. Express* **24**(6), A720–A730 (2016).
11. H. Kogelnik, "Coupled wave theory for thick hologram gratings," *Bell Syst. Tech. J.* **48**(9), 2909–2947 (1969).
12. S. Martin et al., "Holographically recorded low spatial frequency volume Bragg gratings and holographic optical elements," *Holograph. Mater. Opt. Syst.* **4**, 73–98 (2017).
13. W. C. Sweatt, "Describing holographic optical elements as lenses," *JOSA* **67**(6), 803–808 (1977).
14. T. Miyaoka, K. Matsushima, and S. Nakahara, "Optimization of design-wavelength for unobtrusive chromatic aberration in high-definition color computer holography," *Proc. SPIE* **9386**, 93860N (2015).
15. C.-C. Sun, T.-C. Teng, and C.-S. Hsieh, "Wavelength and spatial selectivity of volume holographic optical elements," *Proc. SPIE* **5636**, 289–299 (2005).
16. Covestro GMBH, https://solutions.covestro.com/en/products/bayfol/bayfol-hx200_86194384-20033146?SelectedCountry=US (2018).
17. Bivar. Inc., "Bivar SMS1105 LED technical datasheet," SMS1105PGC PURE GREEN.
18. L. Hwang et al., "Uniformity improvement of a reconstructed-holographic image in a near-eye display system using off-axis HOE," *Opt. Express* **30**(12), 21439–21454 (2022).

Jorge Lasarte is currently a postgraduate student at the Centre for Industrial and Engineering Optics, TU Dublin, Ireland. He received a BSc degree in optics and optometrics from Universidad de Zaragoza in 2019 and an MSc degree in optical and imaging technologies from Universidad Complutense de Madrid in 2021. His current research interests are in developing optical patterning techniques for diffractive optical elements optimized for non-laser sources.

Kevin Murphy is a research fellow and SFI starting Investigator in the Centre for Industrial and Engineering Optics at Technological University Dublin, Ireland. He obtained his PhD in applied optics from the National University of Ireland, Galway (now University of Galway) in 2011. He has more than 15 years experience in optics research across both industry and academia. His research interests are in holographic wavefront sensing, optical vortices, holographic for vision, and photosensitive materials.

Izabela Naydenova is currently the head of Physics and Clinical Measurement Science and scientific director of the IEO Centre, TU Dublin. She was awarded her MSc degree in applied optics from the University of Sofia and her PhD degree in physics from the Bulgarian Academy of Sciences in 1999. Her research interests are in holographic sensing, development of novel holographic recording materials and diffractive optical devices. She was awarded Optica Fellow status in 2023.

Jesús Atencia is senior lecturer in the Faculty of Science, University of Zaragoza, Spain. He received his PhD in the Applied Physics Department, University of Zaragoza, in 1997, with a doctoral thesis on the imaging properties of holographic lenses. His research interests are holography, holographic recording materials, colour holography, and holographic optical elements for specific purposes, as vortex generation, pulse compression, solar concentration, and fiber mode detection

Maria Victoria Collados is senior lecturer in the Faculty of Science, University of Zaragoza, Spain, and coordinator of the Optics and Optometry Program. She received her PhD in the Applied Physics Department, University of Zaragoza, Spain, in 2006, with a doctoral thesis on the application of holographic lenses in achromatic optical processors. Her research interests are holographic optical elements, holographic recording materials, fiber mode detection, and visual optics.

Suzanne Martin is manager for the Centre for Industrial and Engineering Optics at Technological University Dublin, Ireland. She obtained her PhD jointly from Trinity College Dublin and Dublin Institute of Technology, Ireland, in 1996. Her current research interests are in the development of photopolymer materials, fabrication and testing of holographic/diffractive optical elements, design and construction of holographic patterning systems, and modeling diffraction behaviour.